

Effects of Solvents in the Polyethylene Glycol Series on the Bonding of Copper Joints Using Ag₂O Paste

SHINYA TAKATA,^{1,3} TOMO OGURA,¹ EIICHI IDE,² TOSHIAKI MORITA,²
and AKIO HIROSE¹

1.—Division of Materials and Manufacturing Science, Graduate School of Osaka University, 2-1 Yamadaoka, Suita 565-0871, Japan. 2.—Hitachi Research Laboratory, Hitachi Ltd., 7-1-1 Omika, Hitachi 319-1292, Japan. 3.—e-mail: s-takata@mapse.eng.osaka-u.ac.jp

The effects of reducing solvents on the bonding process using silver oxide paste in a copper joint were investigated. Three solvent types were tested: diethylene glycol (DEG), triethylene glycol (TEG), and polyethylene glycol (PEG). The strength of the joints was assessed by fracturing, which occurred at the interface of the copper oxide layer and the copper substrate in DEG and TEG samples and at the bonded interface in the PEG sample. Analysis of the samples revealed that, in the DEG and TEG samples, the copper substrate was oxidized during the bonding process, which compromised the shear strength of the joints. In contrast, the PEG sample exhibited nonuniform sintering of the silver layer while retaining good shear strength. It was found that the combination of DEG and PEG produced optimum shear strength in the copper joint, as PEG suppressed the growth of copper oxide and DEG promoted the formation of a dense sintered silver layer. The bonding strength achieved was higher than that of the gold-to-gold joint made using standard Pb-5Sn solder.

Key words: Ag nanoparticles, Ag oxide, reducing solvent, shear strength, Cu joint

INTRODUCTION

Public concern regarding the environmental impact of heavy metals has grown significantly in recent decades. In 2006, the Restriction of Hazardous Substances (RoHS) directive came into effect, regulating the use of detrimental substances including heavy metals (Pb, Hg, Cd, etc.) commonly used to manufacture electronic products.¹ As a result, the electronics industry has developed lead-free solder for joining together metal components, such as Sn-80Au.^{2–5} However, the use of a noble metal makes this solder rather costly, and alternatives to Pb-5Sn and Pb-10Sn high-temperature solders have not yet been established.

Simultaneously, improvement of energy efficiency has become a top priority, and much attention is

focused on developing semiconductor devices for power conversion in hybrid cars and bullet trains as a strategy for reducing energy usage. Silicon carbide (SiC) has emerged as an attractive power device material, as it possesses the characteristics of low loss, high withstand voltage, and high heat resistance, which permit the reduction of the volume of the semiconductor without decreasing the power. It is expected to be widely applied in hybrid and battery-powered cars because of its excellent performance at high temperatures.^{6–8} Unfortunately, at operating temperatures over 200°C,⁹ solders experience thermal degradation and remelting causes deterioration in strength. Therefore, there is a critical demand for new packaging materials that are lead-free and exhibit improved thermal reliability.

To address these issues, we previously proposed a bonding process using silver metallo-organic nanoparticles.^{10–13} Each particle is covered with organic

(Received May 15, 2012; accepted November 4, 2012;
published online December 11, 2012)

shells composed of higher alcohols, which serve to prevent agglomeration of the silver nanoparticles. During the bonding process, decomposition and discharge of the organic shells occur through heat and pressure, and a dense sintered silver layer is formed by autoagglutination of the silver nanoparticles as their active surfaces are exposed. The process produces a bonding layer made of bulk silver that exhibits high heat and radiation resistance. We confirmed that direct bonding between silver and copper is achieved by the decomposition of copper oxide, which occurs at the same time as the decomposition of the protective organic shells. However, these silver metallo-organic nanoparticles are costly to produce, and cost must be reduced if they are to come into wider use.

As a lower-cost alternative, we have proposed the use of silver oxide particles in the bonding process.^{14–17} Silver oxide particles are reduced by a hydroxyl group of solvent, and produce silver nanoparticles, aldehyde, carbon dioxide, and water steam. Then, almost all aldehyde is burned to carbon dioxide and water steam during heating.¹⁷ These *in situ* generated nanoparticles offer the advantage of low-temperature sinterability and form a dense sintered silver layer. This bonding process is lower in cost because of the use of silver oxide rather than pure silver, and actually provides a higher bonding strength in gold-to-gold and silver-to-silver joints than Pb-5Sn solder. However, we have not yet achieved adequate strength in a copper-to-copper joint using silver oxide particles as a soldering material.

In this study, our objective is to improve the strength of the copper-to-copper joint soldered with silver oxide particles, focusing on optimizing the reducing solvent used in the bonding process. Smaller particles are expected to form a dense sintered silver layer based on reports that reducing solvent affects particle size.^{18,19} Residual organics are thought to reduce the copper oxide to pure copper, and when silver comes into contact with the pure copper it behaves like silver metallo-organic nanoparticles. Therefore, proper selection of the reducing solvent can significantly improve the bonding strength. In this study, we used reducing solvents with different carbon chain lengths and investigated their influence on bondability by observing cross-section and fracture surfaces of each joint.

EXPERIMENTAL PROCEDURES

Silver oxide (Ag_2O) particles of 2 μm to 3 μm diameter were used. The particles were milled using an alumina mortar, mixed with a reducing solvent to concentration of 180 $\mu\text{L/g}$, and processed to paste for bonding. The three types of reducing solvent tested were diethylene glycol (DEG), triethylene glycol (TEG), and polyethylene glycol (PEG), which vary primarily in carbon chain length and molar weight.

A schematic illustration of the shear test sample and method is shown in Fig. 1. A copper substrate was used as the bonded material. The silver oxide paste, prepared with DEG, TEG, or PEG, was applied to the lower substrate using a 50- μm -thick mask and preheated at the optimized conditions in order to remove excess reducing solvent (100°C/5 min for DEG, 120°C/6 min for TEG, and 120°C/10 min for PEG). Subsequently, the upper substrate was placed onto the lower substrate, and the samples were heated to 300°C at a rate of 60°C/min using an infrared heating furnace and held for 5 min at a pressure of 5 MPa. After bonding, the samples were cooled using forced air. The shear strength of the joints was measured using a strain rate of 30 mm/min.

The thermal characteristics of each silver oxide paste were measured with a combination of thermogravimetric (TG) and differential thermal analysis (DTA) at a heating rate of 60°C/min in ambient atmosphere.

The cross-section and fracture surface of each joint was observed by scanning electron microscopy (SEM) and transmission electron microscopy (TEM).

RESULTS AND DISCUSSION

Decomposition Behavior of Silver Oxide Pastes

To investigate the influence of the reducing solvent on the decomposition behavior of silver oxide, the thermal reaction and weight loss upon reduction of the silver oxide was evaluated using TG–DTA, the results of which are shown in Fig. 2. The temperature at which each paste exhibited an exothermal peak accompanied by significant weight loss was different: 119°C for DEG, 140°C for TEG, and 157°C for PEG. The positions of these peaks indicate the formation of silver through the redox reaction between silver oxide and reducing solvent. For the DEG and TEG pastes, all the weight loss occurred during the redox reaction, but for the PEG paste, weight loss continued until the temperature reached 300°C. This weight loss after the redox reaction was completed was likely caused by combustion of residual PEG, which has higher evaporation and combustion temperatures than the other solvents due to its longer carbon chain.

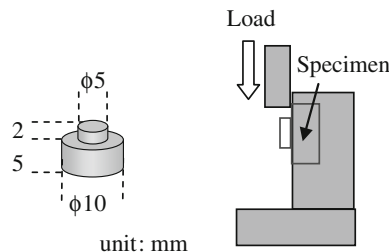


Fig. 1. Schematic illustration of shear test sample and method.

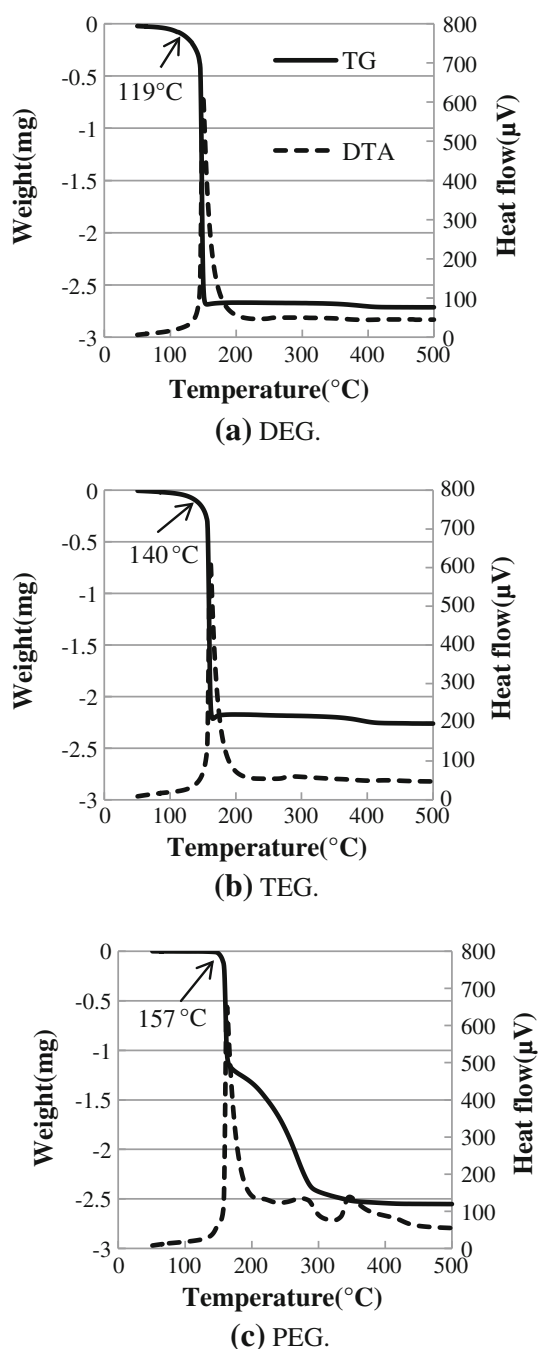


Fig. 2. TG-DTA traces on heating at 60°C/min of silver oxide paste mixed with (a) DEG, (b) TEG, or (c) PEG.

Cross-Section and Interfacial Microstructure of the Joints

SEM images of the cross-section of each joint are shown in Fig. 3. It was found that the thickness and density of the sintered silver layers were different in each sample. The thickness of the silver layers in the DEG and TEG samples was about 20 μm , but that in the PEG sample was only about 5 μm (Fig. 3a, b). In addition, the sintered silver layer in

the PEG sample exhibited large voids and was nonuniform (Fig. 3c-1, c-2). The reducing solvent was sufficiently removed from the silver oxide pastes made with DEG and TEG after preheating, but the paste made with PEG contained too much reducing solvent in spite of optimized preheating. If PEG paste is preheated for longer time, the reduction reaction of silver oxide particles progresses during preheating and the sintering performance is degraded at the bonding process. This resulted in the paste made with PEG being discharged outside the bonded substrates by the applied pressure, and as a result, a thinner and nonuniform layer of silver was formed during bonding.

SEM images of the interface between the sintered silver layer and the copper substrate in each joint are shown in Fig. 4. The intermediate layer, which is assumed to be copper oxide, was observed at the interface in the joints in the DEG and TEG samples (Fig. 4a, b). This layer was clearly observable using TEM; Fig. 5 shows the bonded interface of the joint in the TEG sample. The energy-dispersive spectrometry (EDS) results are presented in Table I, confirming that the intermediate layer was copper oxide, most likely Cu₂O.²⁰ This layer probably results from a natural oxide film on the copper substrate that grew during the bonding process. On the other hand, we could not confirm the composition of the oxide layer in the joint in the PEG sample (Fig. 4c). TG-DTA analysis indicated that some PEG remained after the redox reaction was completed and combusted gradually until the sample reached 300°C (Fig. 2c). Therefore, the oxide film on the copper substrate was reduced by the combustion of PEG, and residual PEG suppressed the oxidation of the copper substrate during bonding.

Shear Strength and the Fracture Surface of the Joints

Figure 6 shows the shear strength measured for the joints prepared with each type of silver oxide paste. The strength increased with the molecular weight of the reducing solvent. The fracture surface after the shear test is shown in Fig. 7, and EDS analysis of the fracture surface is presented in Table II. The fractured surfaces of the joints in the DEG and TEG samples contained black regions, a color which is typically observed on the copper oxide surface. EDS analysis also indicated that the fractured surfaces of the joints in the DEG and TEG samples contained higher amounts of copper and oxygen as compared with the fractured surface of the joint in the PEG sample. In the first two samples, it is possible that the joint is composed of sintered silver under a copper oxide layer. These results suggest that fracture mainly occurred at the copper oxide layer/copper substrate interface in the joints in the DEG and TEG samples, but in the joint in the PEG sample the fracture occurred at the silver layer/copper substrate interface.

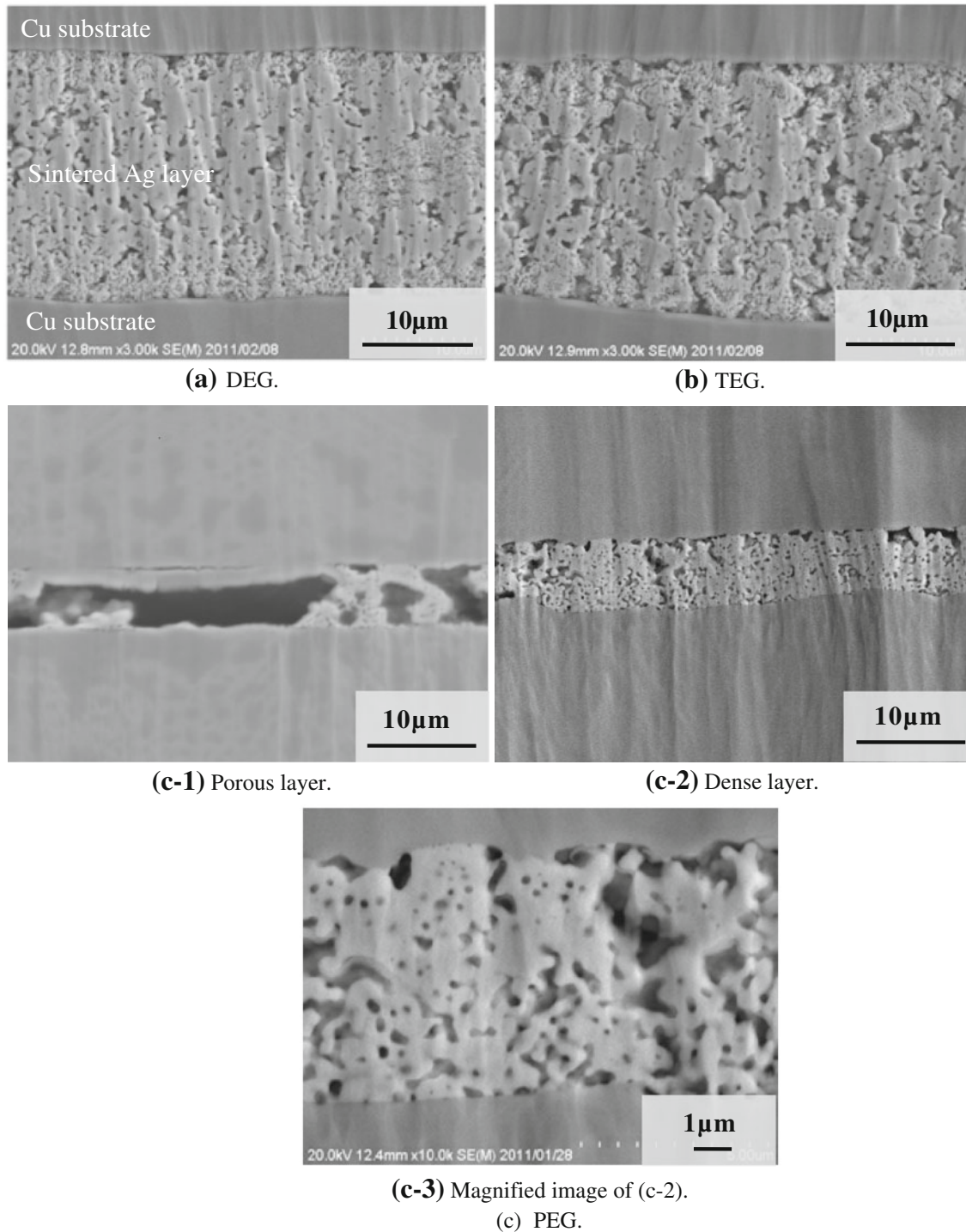
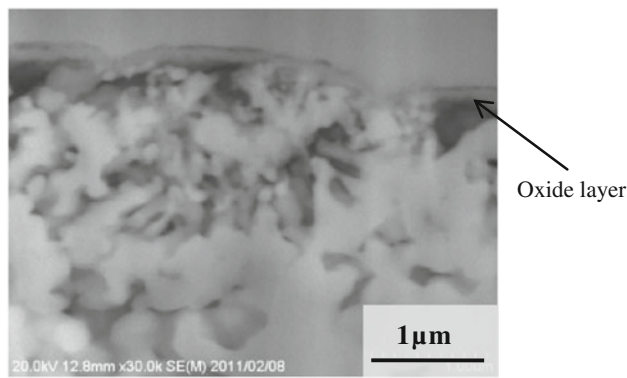


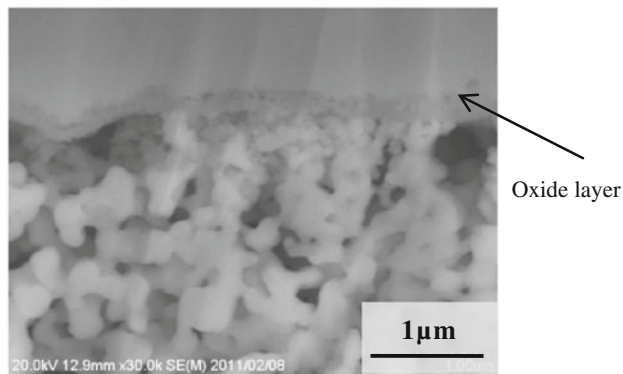
Fig. 3. SEM images of the cross-section of copper-to-copper joints using silver oxide paste mixed with (a) DEG, (b) TEG, or (c) PEG bonded at 300°C for 5 min at pressure of 5 MPa.

Next, we marked off the fracture surface in a reticular pattern and evaluated quantitatively the fracture mode in each region. The area ratio of each fracture mode and the shear strength of each joint are shown in Fig. 8. A total of 73% of the area in the DEG sample and 48% of the area in the TEG sample was fractured between the copper substrate and

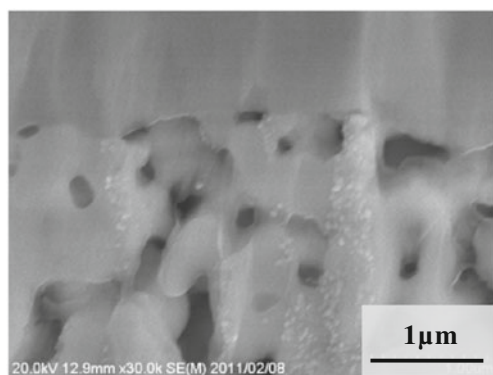
copper oxide layer. In contrast, the entire surface of the joint in the PEG sample was fractured between the sintered silver layer and the copper substrate. The area ratio of fracture is closely related to the shear strength. Consequently, these results indicate that the joints in the DEG and TEG samples had lower bondability because the copper substrate



(a) DEG.



(b) TEG.



(c) PEG.

Fig. 4. SEM images of the copper/silver interface using silver oxide paste mixed with (a) DEG, (b) TEG, or (c) PEG.

oxidized, and the fracture occurred because of the growth of a copper oxide film; however, the joint in the PEG sample exhibited higher bondability because residual PEG suppressed the oxidation of the copper substrate, and the fracture fully occurred at the sintered silver/copper substrate interface.

Effect of DEG/PEG Mixed Solvent on the Bondability of the Joint

These results suggested that PEG suppressed the growth of the copper oxide film and gave rise to higher shear strength of the joint. However, SEM observation showed that PEG also caused nonuni-

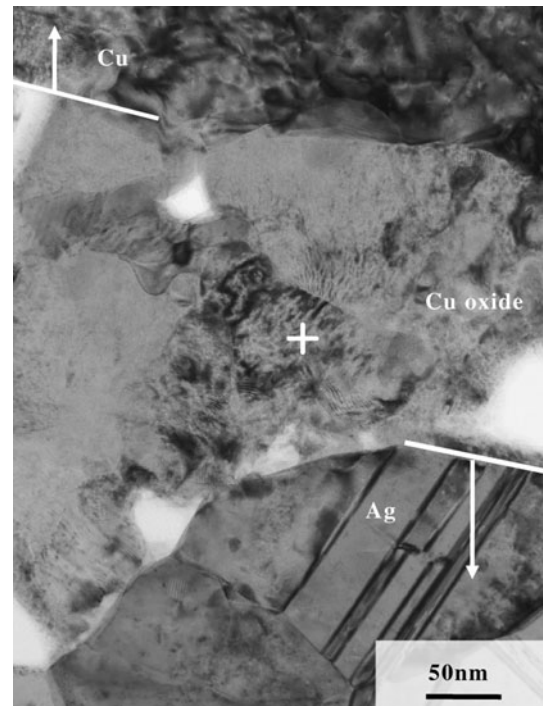


Fig. 5. TEM images of copper/silver interface bonded using silver oxide paste mixed with TEG.

Table I. EDS quantitative analysis at the cross point of the TEM image

Chemical Composition (at.%)

Cu	O
77.1	22.9

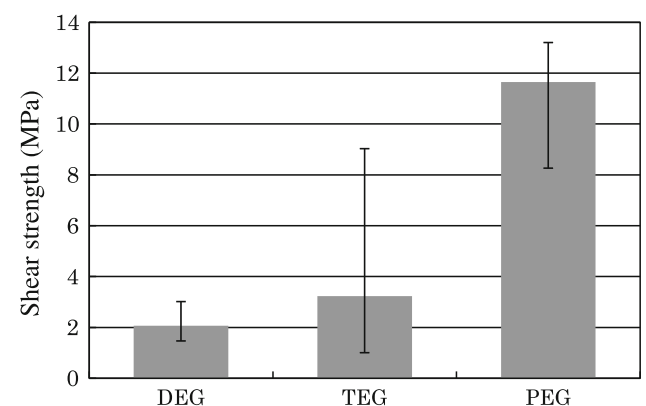


Fig. 6. Shear strength of copper-to-copper joints using silver oxide paste mixed with DEG, TEG, or PEG.

form sintering of the silver layer. On the other hand, the paste made with DEG produced a denser sintered silver layer in the joint. Based on these observations, we decided to test the ability of a

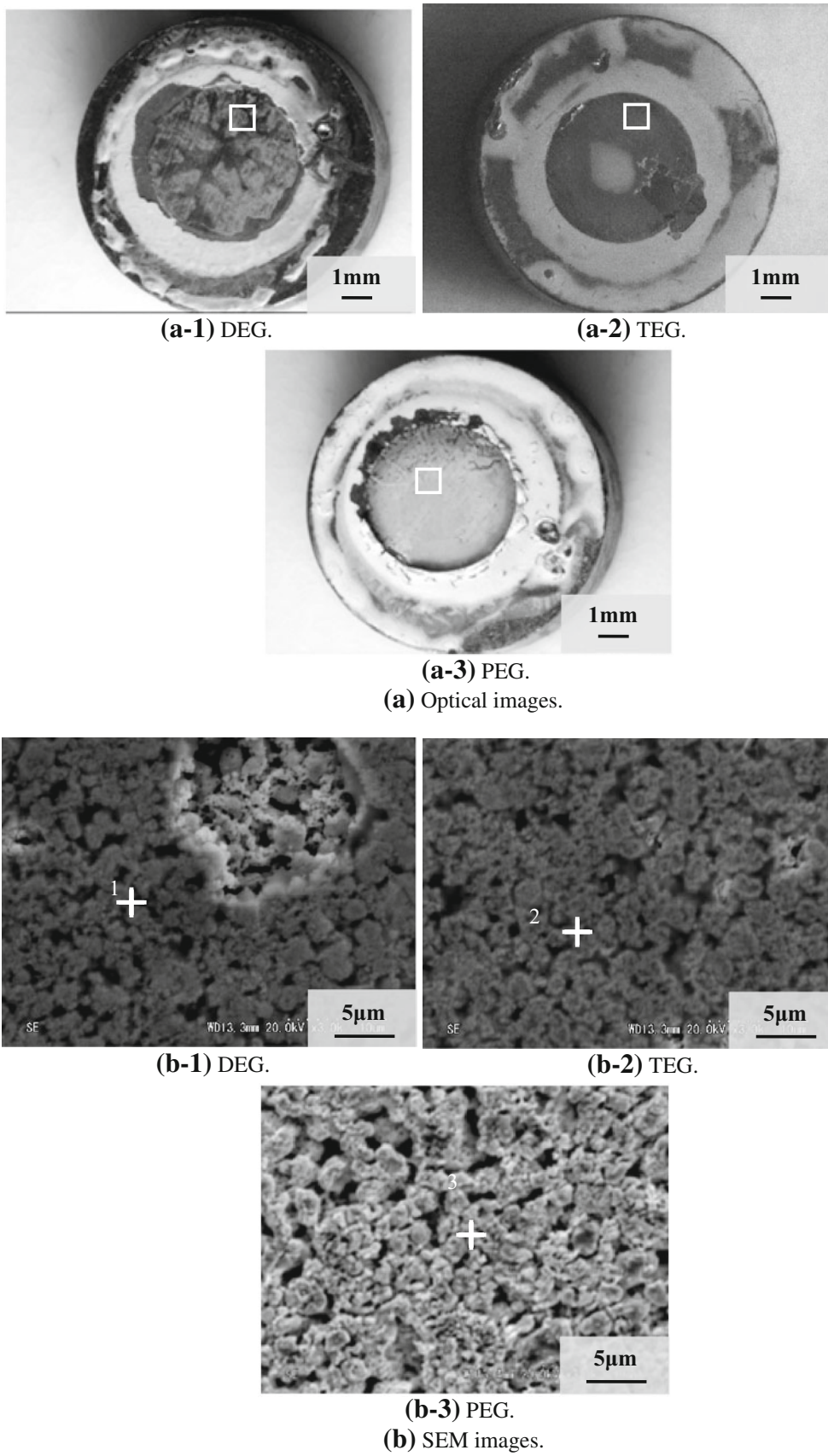


Fig. 7. (a) Optical and (b) SEM images of the fracture surface of copper-to-copper joint using silver oxide paste.

Table II. EDS quantitative analysis of the fracture surface of the joints using silver oxide paste mixed with DEG, TEG, or PEG

Point	Chemical Composition (at.%)		
	Cu	O	Ag
1	12.8	31.1	56.1
2	12.7	37.8	49.5
3	4.7	9.4	85.9

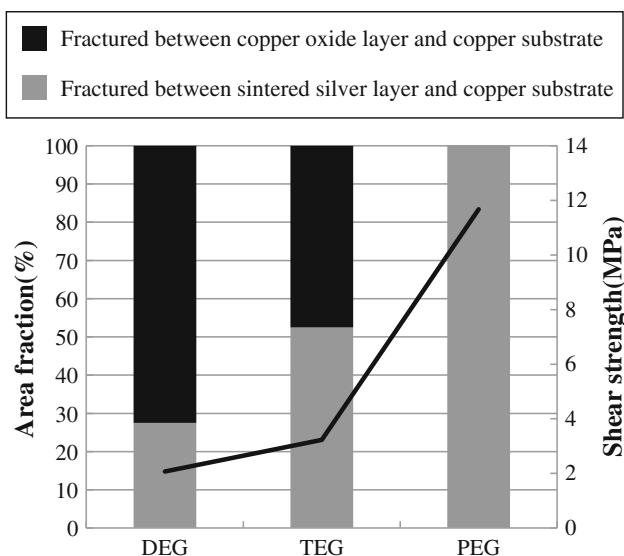


Fig. 8. Area ratio of each fracture mode and shear strength of copper-to-copper joints made with each type of silver oxide paste.

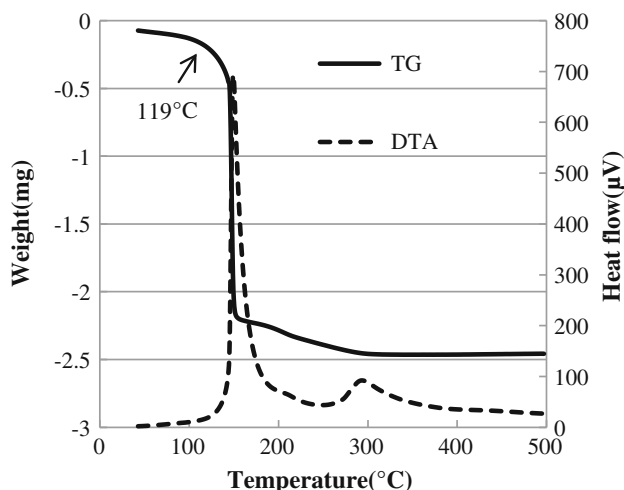


Fig. 9. TG-DTA traces on heating at 60°C/min of DEG/PEG mixed silver oxide paste.

DEG/PEG mixed reducing solvent to improve the bondability of a copper-to-copper joint. In this study, we mixed DEG and PEG in the ratio of 7:3, which

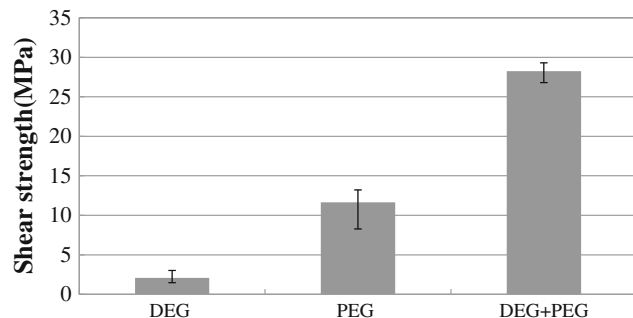
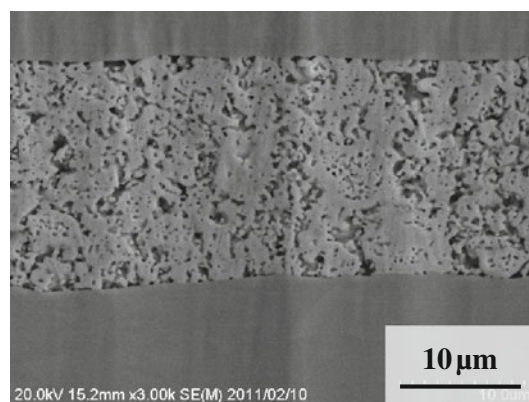
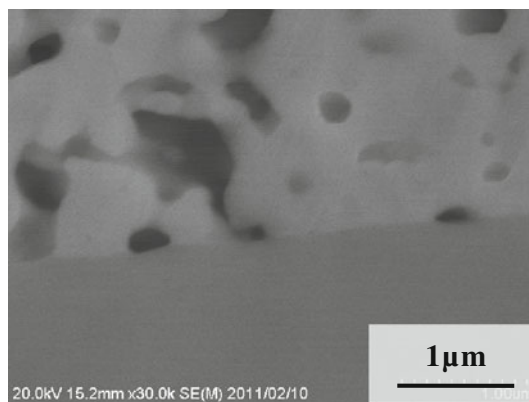


Fig. 10. Shear strength of the copper-to-copper joint using various silver oxide pastes.



(a) General image.



(b) Magnified image.

Fig. 11. SEM images of the copper/silver interface using DEG/PEG mixed silver oxide paste.

was optimized based on several experimental data from our study. A TG-DTA trace of the mixed paste is shown in Fig. 9. The redox reaction between silver oxide and reducing solvent occurred at the onset temperature of DEG, and PEG still remained after the exothermal peak until the temperature reached 300°C, which is the bonding temperature. The shear strength of the joint in the DEG/PEG mixed sample is shown in Fig. 10, reaching a value of 29 MPa. This is higher than that found in gold-to-gold joints

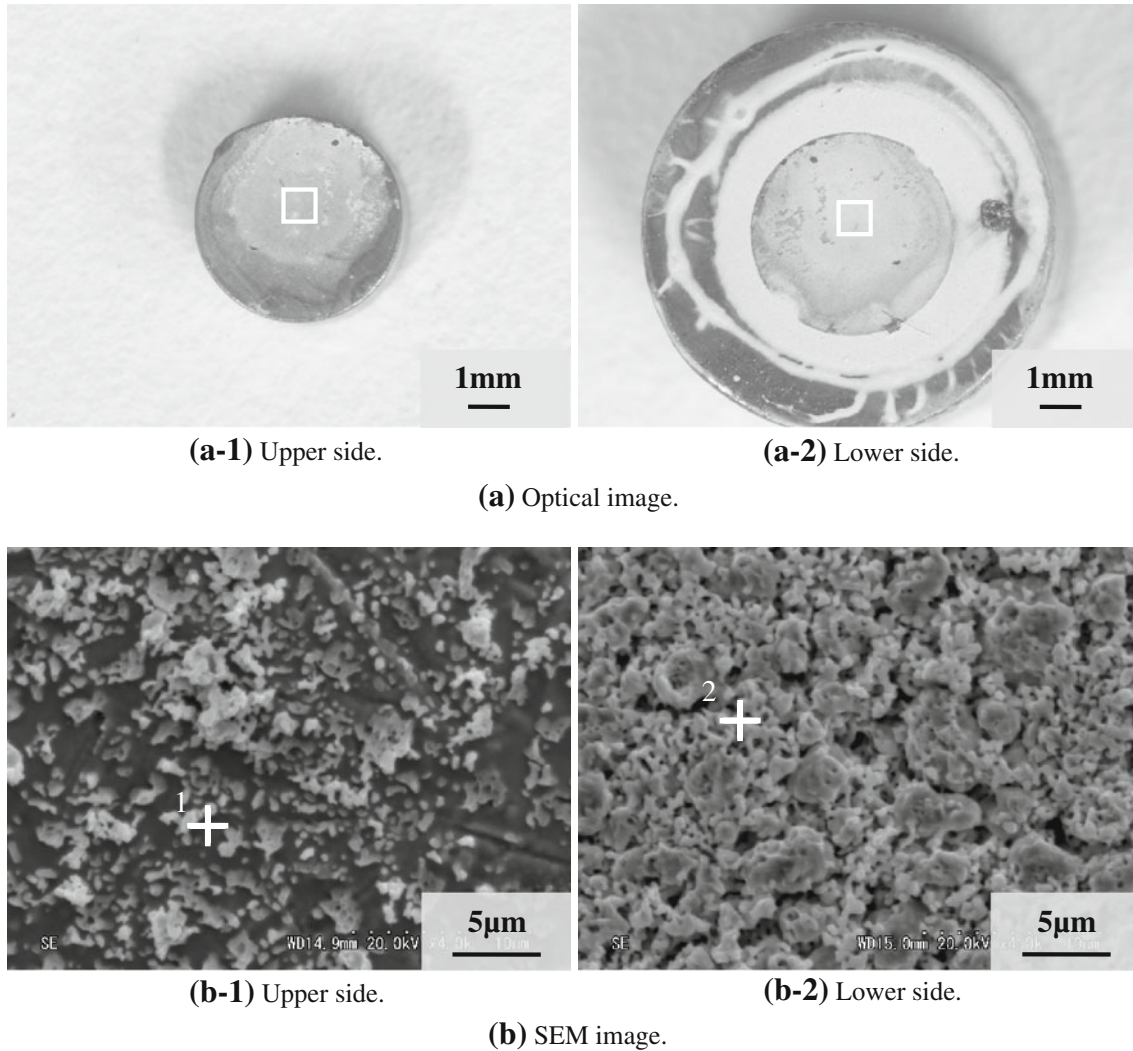


Fig. 12. (a) Optical and (b) SEM images of the fracture surface of copper-to-copper joint using DEG/PEG mixed silver oxide paste.

Table III. EDS quantitative analysis of the fracture surface of the joint using DEG/PEG mixed silver oxide paste

Point	Chemical Composition (at.%)		
	Cu	O	Ag
1	87.6	7.7	4.7
2	1.8	9.4	88.8

made with Pb-5Sn, which is the current industrial standard for die-bonding (~ 18 MPa).¹⁰ This higher strength is explained by the microstructural observations, as shown in Fig. 11. A dense sintered silver layer was formed, and growth of the oxide film was not confirmed. The fracture surface after the shear test is shown in Fig. 12, and EDS analysis of the fracture surface is presented in Table III. EDS analysis showed that the amount of oxygen at the

fracture surface was almost equivalent to that of the PEG sample, and fracture occurred at the dense sintered silver layer/copper substrate interface. This well supports the results of TG-DTA analysis and SEM imaging; that is, the reduction of silver oxide was promoted by DEG, and the growth of oxide film was suppressed by remained PEG. Therefore, it could be concluded that using a mixed reducing solvent containing DEG and PEG gave rise to a copper-to-copper joint with higher strength than that of the gold-to-gold joint made with Pb-5Sn by both promoting the reduction of silver oxide and suppressing the growth of copper oxide at the bonding temperature. Based on these results, we are optimistic that silver oxide paste could be of great use in the bonding process.

CONCLUSIONS

1. Silver oxide particles decomposed to silver via a redox reaction between silver oxide and the

reducing solvent. The onset temperature was different depending on the reducing solvent used. It was found that residual PEG remained until the bonding temperature was reached in the bonding layer after the redox reaction was completed.

2. The copper substrates oxidized during the bonding process in both the DEG and TEG samples, but no copper oxide was found in the PEG sample. Fracture mainly occurred by peeling of the oxide films in DEG and TEG samples, but the entire surface of the joint was fractured at the bonded interface in the PEG sample.
3. The shear strength was improved by both promoting the reduction of silver oxide and suppressing the growth of copper oxide at the bonding temperature by combining DEG and PEG in a mixed paste.
4. The DEG/PEG mixed solvent gave rise to a copper-to-copper joint with higher strength than that of the gold-to-gold joint made with Pb-5Sn, suggesting that silver oxide paste could be an alternative to lead-free soldering.

ACKNOWLEDGEMENT

This work was supported by a Grant-in-Aid for Scientific Research (B) No. 23360322, Japan, and by Priority Assistance for the Formation of Worldwide Renowned Centers of Research—The Global COE Program (Project: Center of Excellence for Advanced Structural and Functional Materials Design) from the Ministry of Education, Culture, Sports, Science, and Technology (MEXT), Japan.

REFERENCES

1. K.J. Puttlitz and G.T. Galyon, *J. Mater. Sci.: Mater. Electron.* 18, 347 (2007).
2. V. Chidambaram, J. Hattel, and J. Hald, *Microelectron. Eng.* 88, 981 (2011).
3. J.W. Ronnie Teo, F.L. Ng, L.S. Kip Goi, Y.F. Sun, Z.F. Wang, X.Q. Shin, J. Wei, and G.Y. Li, *Microelectron. Eng.* 85, 512 (2008).
4. G.S. Zhang, H.Y. Jing, L.Y. Xu, J. Wei, and Y.D. Han, *J. Alloys Compd.* 476, 138 (2009).
5. Y.C. Liu, J.W.R. Teo, S.K. Tung, and K.H. Lam, *J. Alloys Compd.* 448, 340 (2008).
6. R.R. Siergiej, R.C. Clarke, S. Sriram, A.K. Agarwal, R.J. Bojko, A.W. Morse, V. Balakrishna, M.F. MacMillan, A.A. Burk Jr, and C.D. Brandt, *Mater. Sci. Eng.* 61–62, 9 (1999).
7. M. Hasanuzzaman, S.K. Islam, L.M. Tolbert, and M.T. Alam, *Solid-State Electron.* 48, 1877 (2004).
8. M. Hasanuzzaman, S.K. Islam, and L.M. Tolbert, *Solid-State Electron.* 48, 125 (2004).
9. K. Sheng, L.C. Yu, J. Zhang, and J.H. Zhao, *Solid-State Electron.* 50, 1073 (2006).
10. E. Ide, A. Hirose, and K.F. Kobayashi, *Mater. Trans.* 47, 211 (2006).
11. T. Morita, E. Ide, Y. Yasuda, A. Hirose, and K. Kobayashi, *Jpn. J. Appl. Phys.* 47, 6615 (2008).
12. Y. Akada, H. Tatsumi, T. Yamaguchi, A. Hirose, T. Morita, and E. Ide, *Mater. Trans.* 49, 1537 (2008).
13. T. Morita, Y. Yasuda, E. Ide, Y. Akada, and A. Hirose, *Mater. Trans.* 49, 2875 (2008).
14. A. Hirose, H. Tatsumi, N. Takeda, Y. Akada, T. Ogura, E. Ide, and T. Morita, *J. Phys: Conf. Ser.* 165, 012074 (2009).
15. T. Morita, Y. Yasuda, E. Ide, and A. Hirose, *Mater. Trans.* 50, 226 (2009).
16. T. Ogura, M. Nishimura, H. Tatsumi, N. Takeda, W. Takahara, and A. Hirose, *Open Surf. Sci. J.* 3, 55 (2011).
17. T. Morita, Y. Yasuda, E. Ide, and A. Hirose, *J. Jpn. Inst. Electron. Packag.* 12, 110 (2009).
18. C. Luo, Y. Zhang, X. Zeng, Y. Zeng, and Y. Wang, *Colloid Interface Sci.* 288, 444 (2005).
19. H. Suk Shin, H.J. Yang, S.B. Kim, and M.S. Lee, *Colloid Interface* 274, 89 (2004).
20. A. Njeh, T. Wieder, and H. Fuess, *Surf. Interface Anal.* 33, 626 (2002).